aerospace

MDPI

Article

Wing Structure of the Next-Generation Civil Tiltrotor: From Concept to Preliminary Design

Marika Belardo [1,*], Aniello Daniele Marano [2], Jacopo Beretta [3], Gianluca Diodati [1], Mario Graziano [4], Mariacarmela Capasso [4], Pierpaolo Ariola [5], Salvatore Orlando [5], Francesco Di Caprio [1], Nicola Paletta [3] and Luigi Di Palma [1]

1 Italian Aerospace Research Centre (CIRA), 81043 Capua, Italy; g.diodati@cira.it (G.D.); f.dicaprio@cira.it (F.D.C.); l.dipalma@cira.it (L.D.P.)
2 Department of Industrial Engineering, University of Naples Federico II, 80125 Napoli, Italy; aniellodaniele.marano@unina.it
3 IBK-Innovation GmbH, 21129 Hamburg, Germany; jacopo.beretta@ibk-innovation.de (J.B.); nicola.paletta@ibk-innovation.de (N.P.)
4 Step Sud Mare Srl, 80038 Pomigliano d'Arco, Italy; mario.graziano@stepsudmare.com (M.G.); mariacarmela.capasso@stepsudmare.com (M.C.)
5 Magnaghi Group S.p.A, 80146 Napoli, Italy; pariola@magroup.net (P.A.); sorlando@magroup.net (S.O.)
* Correspondence: m.belardo@cira.it

Abstract: The main objective of this paper is to describe a methodology to be applied in the preliminary design of a tiltrotor wing based on previously developed conceptual design methods. The reference vehicle is the Next-Generation Civil Tiltrotor Technology Demonstrator (NGCTR-TD) developed by Leonardo Helicopters within the Clean Sky research program framework. In a previous work by the authors, based on the specific requirements (i.e., dynamics, strength, buckling, functional), the first iteration of design was aimed at finding a wing structure with a minimized structural weight but at the same time strong and stiff enough to comply with sizing loads and aeroelastic stability in the flight envelope. Now, the outcome from the first design loop is used to build a global Finite Element Model (FEM), to be used for a multi-objective optimization performed by using a commercial software environment. In other words, the design strategy, aimed at finding a first optimal solution in terms of the thickness of composite components, is based on a two-level optimization. The first-level optimization is performed with engineering models (non-FEA-based), and the second-level optimization, discussed in this paper, within an FEA environment. The latter is shown to provide satisfactory results in terms of overall wing weight, and a zonal optimization of the composite parts, which is the starting point of an engineered model and a detailed FEM (beyond the scope of the present work), which will also take into account manufacturing, assembly, installation, accessibility and maintenance constraints.

Keywords: civil tiltrotor; wing; design; aeroelasticity; flutter; multi-objective optimization

Citation: Belardo, M.; Marano, A.D.; Beretta, J.; Diodati, G.; Graziano, M.; Capasso, M.; Ariola, P.; Orlando, S.; Di Caprio, F.; Paletta, N.; et al. Wing Structure of the Next-Generation Civil Tiltrotor: From Concept to Preliminary Design. *Aerospace* **2021**, *8*, 102. https://doi.org/10.3390/aerospace8040102

Academic Editor: Christian Breitsamter

Received: 2 March 2021
Accepted: 29 March 2021
Published: 2 April 2021

1. Introduction

Tiltrotors are a class of vehicle that combines the advantages of aircraft (high cruise speed) and helicopters (Vertical Take-Off and Landing (VTOL) ability). Their commercial appeal is becoming increasingly important, with applications among various users, such as business, search and rescue, and medical. Within this framework, Horizon 2020 (H2020) Clean Sky 2 FRC IADP NextGenCTR will be dedicated to the design, construction and flying of an innovative Next-Generation Civil Tiltrotor Technology Demonstrator (NGCTR-TD) [1], the configuration of which will go beyond current architectures for this type of aircraft. NGCTR-TD demonstration activities, led by Leonardo Helicopters Division (LHD), will aim to validate its innovative architecture, technologies/systems and operational concepts.

The NGCTR-TD (https://www.cleansky.eu/fast-rotorcraft-iadp (accessed on 1 April 2021)) is characterized by a 12 m long wing, a V-Tail, pitch and yaw lift surfaces' command configuration, and a fixed-engine installation with a split gearbox to provide the proprotor tilting mechanism.

The T-WING consortium is working on the composite wing of the NGCTR-TD, planned to be flying in 2023. The consortium, led by the Italian Aerospace Research Centre (CIRA), is composed of industrial partners Magnaghi Aeronautica and Salver (IT) and SSM (IT), small and medium-sized enterprises (SMEs) OMI (IT) and IBK Innovation (DE), and the University of Naples Federico II (IT). The final aim of the project is to design and qualify the structure of the wing and moveable surfaces, encompassing from design, manufacturing and ground tests up to flight, in compliance with the technical specification set by the Work Area Leader Leonardo Helicopters. The wing will be properly instrumented during the flight, with a set of sensors (strain gages and accelerometers) with the aim of validating load evaluation methods, structural monitoring for flight safety and aeroelastic characteristics.

The main innovations pertaining to the wing structure are the highly integrated composite concept and the presence of two moveable surfaces: one is an external flaperon and the other is a so-called morphing surface, which has the function of reducing the wing area exposed to the propeller flow in helicopter mode. All these features lead to a wing structure which is quite compact, since the largest moveable surface spans almost half of the wing chord.

For such a wing, an iterative and novel optimization process has been necessary, even if the architectural layout of the structure is set by LHD (e.g., spar and ribs locations). The optimization process was thus aimed at finding the optimal composite thickness distribution (at minimum weight). In the present case of the NGCTR-TD wing, the preliminary structural design strategy is based on a two-level optimization. The first-level optimization, presented in a previous work by the authors [1], is based on engineering models, used to perform a multi-objective optimization by means of genetic algorithms, also taking into account the aeroelastic stability. The aim of the first-level optimization is to have, at the very beginning of the project, i.e., at concept design level, a safe structural configuration, which is free from flutter at minimum mass. The second-level optimization is based on a 2D-1D elements Finite Element Model (FEM), built based on the selected first-level structural optimization [2]. The composite parts (skin and spars) of this structural configuration are then subjected to optimization by means of commercial FEM software (OptiStruct®, ver. 2017.2, Altair Engineering Inc., Troy, MI, USA). In order to speed up the optimization process and to evaluate different design choices, the equivalent laminate theory is applied to model the composite properties of the finite elements, also giving an advantage in the computational effort. The second-level optimization is the main object of the present work.

2. Previous Similar Works

A remarkable example of a design optimization framework for a tiltrotor wing is about the SUAV TRS4 composite wing [3], in which the mathematical optimization process, based on a gradient-based method and a Variation Asymptotic Beam Sectional (VABS) analysis, was performed by implementing numerical analysis modules, in a single MATLAB® (ver. R2017b, MathWorks, Natick, MA, USA) environment.

Another literature example of tiltrotor wing structural optimization is presented in [4], in which the use case was the Bell XV-15 Tiltrotor, manufactured by the US Bell Aircraft Corporation (Buffalo, NY, USA), predecessor of Bell Helicopter Textron. In this work, the enhancement of the aeroelastic stability is selected as an objective in the upper-level optimization, in which the Response Surface Method (RSM) is selected. On the other hand, lower-level optimization seeks to determine the local detailed cross-sectional parameters, such as the ply orientation angles and ply thickness, which are relevant to the wing structural properties obtained at the upper level. To avoid manufacturing difficulties, only a few discrete ply orientation angles and an integral number of plies are considered as

constraints. A genetic algorithm is selected as the optimizer at the lower level. Finally, a Korea Aerospace Research Institute (KARI) in-house aeroelastic analysis is carried out in order to predict flutter stability.

In the present work, the geometrical constraints of the wing architecture are dictated by LHD; thus, the design variables taken into account for the optimization of the wing-box are mainly the thicknesses/layups of the composite material. The composite material is an already certified material owned by one partner of the T-WING consortium. The aeroelastic problem considered in the optimization is related to the flutter, whereas the whirl flutter is treated as an ex post verification by LHD. The sizing loads are supplied by LHD as well. The aeroelastic behavior is influenced not only by the wing stiffness itself, but also by the local stiffness of the junctions, in this case the junction between the wing and the nacelles. This behavior was already found by the authors in a previous work on a joined fixed-wing configuration [5,6].

The first-phase optimization of the NGCTR-TD wing has already been performed by the authors and briefly recalled in this paper.

3. Requirements and Design Strategy

For the NGCTR-TD, the requirements derived from airworthiness specifications are drawn from EASA (European Aviation Safety Agency) large airplanes (CS-25) and large rotorcrafts (CS-29), for the particular nature of the vehicle. In addition to that, tailored requirements are necessary, since not all the airplane and rotorcraft requirements encompass all the possible scenarios which characterize the tiltrotor. Regarding the structural architecture, as mentioned before, LHD has fixed a number of technical and functional requirements, which have as an outcome a prescribed position of the spars, ribs and moveable surfaces' geometry. As an example, the fuel capacity of the vehicle is a crucial aspect, which dictates the space available for the fuel bladders (fuel is stored in bladders to cope with crashworthiness requirements), whereas the remaining systems (hydraulics, electrical and avionics equipment, the control surface actuators and the Inter-Connecting Drive Shaft, ICDS) are hosted in the wing-box according to segregation requirements. Given the architecture, the wing structural design, in terms of skin and spar web thicknesses and stringers and spar cap areas, has to cope with strength and buckling requirements, at the lowest possible weight, and more predominantly, with stiffness requirements. Stiffness requirements are of paramount importance when designing the wing of a tiltrotor, making the task quite challen ging also in view of other requirements such as the weight and the accessibility (numerous and wide access holes and removable panels, which tend to reduce torsional stiffness). Stiffness requirements are expressed in terms of limitations on the frequency values of the airframe elastic modes. In particular, for the NGCTR-TD wing, airframe modes that involve significant movement of the hub center in the rotor disc plane directions shall have frequencies falling outside "forbidden bands", and in order to avoid whirl flutter stability issues, further limits (minimum values) are imposed on some elastic modes' frequencies, such as torsion modes [7–11]. There is also a requirement on the lowest elastic airframe mode frequency, which shall not be lower than a minimum value, in order to avoid coupling with aeromechanical modes—this is quite demanding when dealing with big masses at the wing tip (nacelles, engine and propellers).

Based on the abovementioned requirements, the design strategy in the preliminary phase is composed of two main phases/levels as shown in Figure 1.

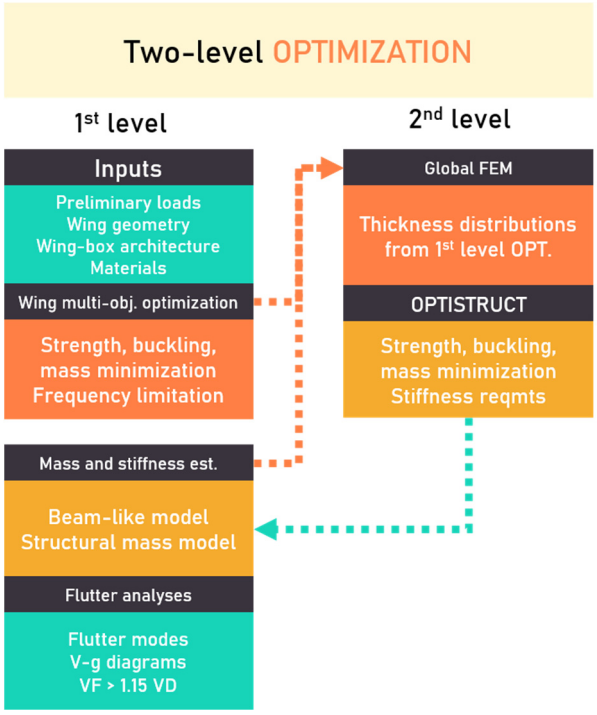

Figure 1. Design strategy flowchart.

The first level consists in a multi-objective optimization (M-OO), looped with aeroelastic analyses, performed with MSC Nastran (ver. 2013.1, MSC Software, Newport Beach, CA, USA). It mainly consists of Matlab in-house codes (based on classical shear flow formulas in closed thin-walled sections and panel buckling formulas), which allow the performance of optimization runs in a very short time (compared with Finite Element Analysis) with an acceptable degree of fidelity. The process aim is to find a set of feasible web/skin thicknesses and spar cap areas compliant with the strength and structural dynamics requirements, with the lowest possible structural mass. In this manner, a first composite wing structure, able to withstand preliminary sizing loads, and free from flutter within the flight envelope, is obtained [11]. Starting from the solution identified in the first-level optimization, the models are updated to allow calculation of updated loads and to compute again flutter speed.

The second level consists in a Finite Element-based multi-objective optimization within an Altair OptiStruct environment. In particular, the optimization is performed for the composite elements (skins and spars), in order to find the best solution—in terms of thickness—which minimizes the structural weight and is compliant with strength and buckling requirements and mainly with the stiffness (flexural and torsional), which is a design driver for a tiltrotor wing. The Finite Element model of the wing is mainly built with 2D and 1D elements (composite 2D elements modeled with equivalent shells based on the classical lamination theory). The optimization constraints are no buckling up to a predefined percentage of limit load (no buckling up to 80% $\times$ LL for the skin; up to 130% $\times$ LL for the spars), positive margins of safety at ultimate load, and minimum flexural (in-plane and out-of-plane) and torsional stiffness. The algorithm is a gradient descent optimization. The design variables of this optimization process are the thicknesses of the upper and lower skins and of the spars, all made of carbon fiber-reinforced plastic. The outcome is a zonal optimization along the wingspan. The optimized FEM will be used to compute new stiffness distributions, then to update the structural aeroelastic stick beam model and to repeat analyses. Moreover, this zonal optimization is the starting point of a detailed FEM, which will also take into account manufacturing, assembly, installation, accessibility and maintenance constraints, and which is beyond the scope of the present work.

3.1. Materials and Methods

The aim of the optimization is to find the best solution from a set of feasible solutions to a problem. In structural optimization, the kind of optimization applied in the present work, typical problems are sizing optimization, shape optimization and topology optimization. As already reported in the previous section, a two-phase/level structural optimization method was needed for this application. The first one makes use of 1D beam theory to achieve the best wing-box thickness distributions able to cope with different load conditions encountered in-flight by the aircraft and respecting flutter stability; the second one is a refinement based on the use of a more accurate models, based on finite elements. The first-level optimization phase rapidly spans the variable space, through an evolutionary genetic algorithm, in order to highlight the variable space zone with best performances (in terms of stress, buckling and stiffness properties). The second-level optimization makes use of a more efficient but local optimization algorithm, to identify the best wing-box candidate satisfying, from an FE model point of view, the requirements (only the structure thickness is varied during the optimization process) starting from the good starting solutions highlighted during the first phase.

3.1.1. Genetic Algorithm Multi-Objective Optimization Approach (First Phase)

A Multi-Objective Genetic Algorithm optimization was used to optimize the wing-box structure [12]. The Genetic Algorithm is a stochastic algorithm that simulates the mechanism of natural evolution by applying the principle of survival in order to produce and obtain improved approximations to a solution. Individuals are encoded as strings, chromosomes: Chromosome values (the genotype) are uniquely mapped to the design variables (96 wing-box thicknesses in our problem, the wing-box phenotype).

From the phenotype it is possible to assess the performance of the wing-box represented by a certain chromosome by calculating the mass and the performance of the wing-box—its fitness values. Once the individuals have been assigned a fitness value, they can be chosen from the population, with a probability according to their relative fitness. The best individuals have more chances to transmit their genetic heritage to future generations. Then they are recombined (by choosing parts from their chromosome, and thus from their wing-box thickness distribution) to produce the next generation. The Genetic Algorithm selects a number of individuals inside the current population, called "parents", and uses them to create the individuals of the next generation called "offspring" or "children". The performance of individuals in a population tends to increase generation by generation, and the Genetic Algorithm (GA) is terminated when one or more pre-fixed criteria are satisfied.

During evolution guided by GAs, non-dominated optimal solutions that identify a Pareto front [13,14] can be recognized, and a solution which best fits the requirements can be chosen by performing an a posteriori trade-off between non-dominated solutions.

The optimization objectives (wing mass, strength and buckling) together with the stress and stiffness properties of the wing are calculated through an in-house code, written in Matlab language, according to bending and shear stress analysis of the wing from engineering manuals [15].

Input data for the program include wing geometrical and airfoil shapes, wing-box architecture (positions of the cross-sectional structural elements), wingspan loads, material data, and initial guess values for skin thickness and spar cap areas. Output data include internal stresses, wing structural mass estimation, and stiffness properties of the wing at selected span locations.

The output stresses are used to calculate strength and buckling Margins of Safety (MS). A solution is considered feasible if all strength and buckling MS are ≥ 0.

3.1.2. Aeroelastic Model

The first level optimization activity, among the other outputs, gives the wingspan beam stiffness and structural mass distribution, which is used to build the dynamic part of the aeroelastic model, Figure 2.

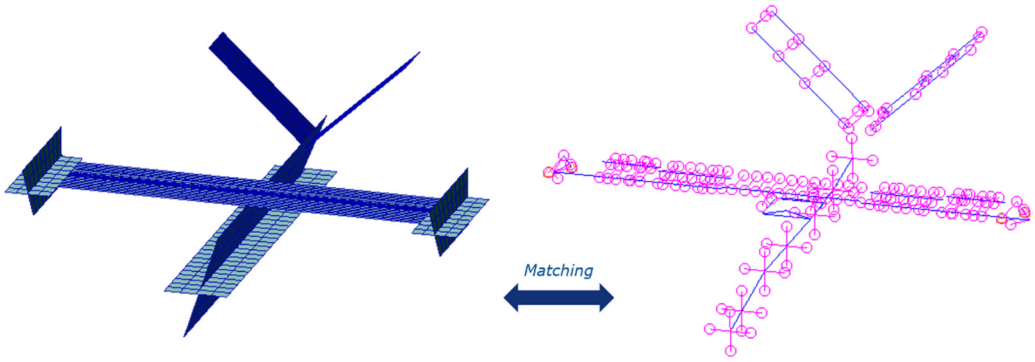

Figure 2. Aeroelastic model.

The model takes into account—concerning structural dynamics—all the parts of the vehicle, not only the wing and moveable surfaces (represented as beam-like models). The remaining tiltrotor parts were supplied as Nastran super-elements by LHD (e.g., fuselage, nacelles, vertical tail and junction between the wing and the fuselage). The kinematics of the moveable surfaces' actuation chains are simulated by means of connection elements of suitable stiffness. The mass model consists in lumped masses (structural and non-structural) along the wingspan. The wing structural masses are an output of the first-level structural design optimization, whereas non-structural masses encompass fuel, fuel system, ICDS, hydraulics system, electrical cables, actuators. The aerodynamic model has been realized according to the Doublet Lattice Method [16,17]. This aerodynamic method, based on the linearized potential flow aerodynamic theory, is the extension to unsteady flows of the simple and steady Vortex Lattice Method. Aerodynamic flat panels are on the wing and tail, whereas perpendicular flat panels simulate fuselage and nacelles, by creating crosses, in order to better represent, in addition to the vertical aerodynamic contribution, the lateral aerodynamic loads induced by the volumetric shape of the abovementioned components. Infinite Plates Spines [18,19] assure the matching between dynamics and aerodynamics.

3.1.3. Size Optimization with FEM (Second Phase)

ALTAIR Hyperworks OptiStruct [20] has the capability of performing size optimization, the type of optimization suitable for the problem in hand. In size optimization, the shape of the structure is known and the properties of structural elements such as shell thickness, beam cross-sectional properties, spring stiffness, and mass are modified to solve the optimization problem. In the present work, the thicknesses of 2D FEM elements are used as optimization variables to search for an optimized structure: thickness variation during optimization is taken by OptiStruct as continuous. Each size variable is defined by using a DESVAR (DESign VARiables) bulk data entry. The DESVAR cards are related to size properties in the model using a DVPREL1 bulk data entry (these cards teach the solver how to link the design variables—one or more—to FEM properties used by the FE solver). Different responses can be set in OptiStruct as design goals, as shown in Table 1. Buckling factor and static stress/strain are of interest for the present method. There are many different methods or algorithms that can be used to optimize a structure. In OptiStruct, algorithms based on the gradient method for size (and shape) optimization are implemented. For this class of methods, the quality of the starting design is a very important component of the process: The probability of finding at least one optimal local representative of the best possible solution is higher when the distance between the initial design parameters and the global optimum is kept as small as possible based on engineering judgement or previous global optimizations [21].

Table 1. Optistruct design goals and functionalities.

Mass	Volume	Center of Gravity
Moment of Inertia	Static Compliance	Static Displacement
Natural Frequency	Buckling Factor	Static Stress, Strain, Forces
Static Composite Stress, Strain, Failure Index	Frequency Response Displacement, Velocity, Acceleration	Frequency Response Stress, Strain, Forces
Weighted Compliance Function	Weighted Frequency	Combined Compliance Index
	Temperature	

As gradient search methods are iterative procedures, it is necessary to instruct the optimizer on how long to search by imposing the maximum number of iterations. Further, it is necessary to specify how fine the search must be: If the difference between two consecutive proposals is less than a convergence tolerance, acceptable from a design perspective, the optimizer concludes the job. Before starting the optimization, OptiStruct performs a design sensitivity analysis of the structural responses (with respect to the design variables) to maximize the efficiency of the optimization process [22].

3.1.3.1. Structural Finite Element Model—Starting Model

The Nastran FEM used for the optimization was primarily built to allow for strength and buckling verification in the preliminary design phase. The model is a Global FEM, meaning that it also comprises the remaining subsystems of the vehicle as super-elements or concentrated masses (i.e., fuselage, wing tip nacelles, tail, systems hosted in the wing, fuel mass). Analyses are performed by activating the INERTIA RELIEF option with SUPORT at aircraft Center of Gravity (CoG). The wing FE model is shown in Figure 3. It is characterized by 2D (TRIA and QUAD) elements for the wing's upper and lower skin, stringers, spar webs and ribs; and by 1D (CROD) elements for caps. RBE3 elements have the function of transferring loads to the structure (inertial; aerodynamics). Suitable RBE2 elements simulate the structural links at the wing–fuselage junction.

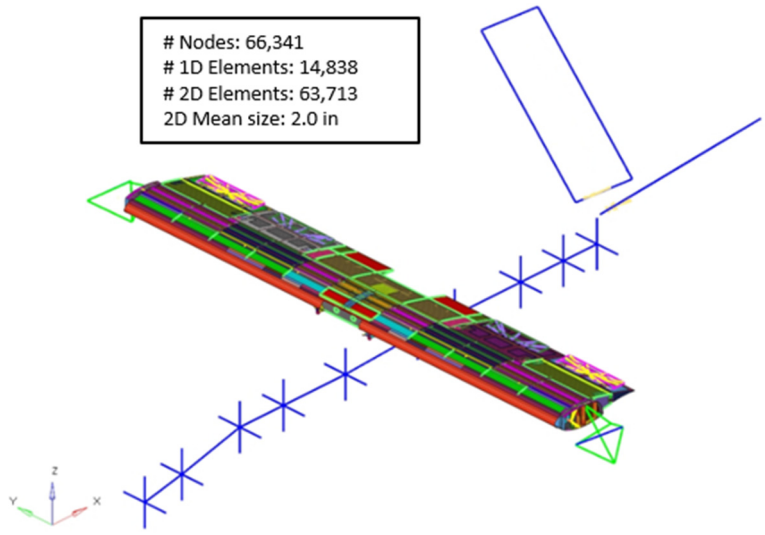

Figure 3. Global Finite Element Model (FEM).

For composite element properties, PCOMP cards and 2D orthotropic material MAT8 are used. PSHELL and MAT1 cards are for isotropic material parts. The sizing load conditions are a number of 50 conditions, which comprise aerodynamic loads, propulsion forces at nacelle prop-rotor location and inertia loads.

3.1.3.2. Materials

The main wing components (i.e., spars, skins, shape ribs) are designed in carbon fiber-reinforced plastics, while the end ribs and ribs joined to the wing–fuselage links are designed in aluminum alloy. Tables 2 and 3 show the properties used for the optimization phases.

Table 2. Composite material properties [23].

Properties	Direction	Modulus	RTD Value (MPa)	Density (Kg/m^3)	Cured Ply Thickness (mm)
Tension	0	E_{11}	59,777	1520	0.31877
Compression	0	$-E_{11}$	55,916		
Tension	90	E_{22}	58,053		
Compression	90	$-E_{22}$	55,020		
Shear	-	G_{12}	3930		
Poisson ratio	-	ν_{12}	0.056		

Table 3. Aluminum alloy 7050 (room temperature values).

Properties	Direction (°)	Modulus (GPa)	Tensile Strength (MPa)	Density (Kg/m^3)	Yield Strength (MPa)
Tension	0, 90	71	525	2750	470
Shear	-	26.5	-		
Poisson ratio	-	0.33	0.056		

3.1.3.3. Loads

The loads provided by the vehicle manufacturer are in terms of accelerations and rates at vehicle CoG plus the corresponding aerodynamic pressures, balancing loads and concentrated loads such as the prop-rotor thrusts. Two sets of load cases are provided: twenty-five sizing loads conditions at International Standard Atmosphere (ISA) ambient condition, plus an additional twenty-five sizing conditions at $-45°$ Outside Air Temperature (OAT) ambient condition (cold day). The load conditions are employed to load the wing FEM model and the remainder of the vehicle in order to perform inertial relief analysis on the whole tiltrotor (each load condition determines fully balanced vehicle conditions). Preliminary MSC Nastran static analysis was performed in order to calculate the shear/bending/torsion diagrams along the wing and to identify the most critical load conditions to be used in the optimization FE loop. Each set contains 25 load cases, encompassing ground (e.g., taxi, turning, brake roll, landing), flight maneuvers both in helicopter and aircraft modes (e.g., symmetric pull-up, symmetric push-over, yaw, rolling) and gust conditions. For the case under study, the most demanding load conditions have been proven to be LC09 (low speed pull-up maneuver in helicopter mode) and LC12 (Taxi). In the Figures 4 and 5, the wing internal loads diagram of the most demanding load conditions are presented.

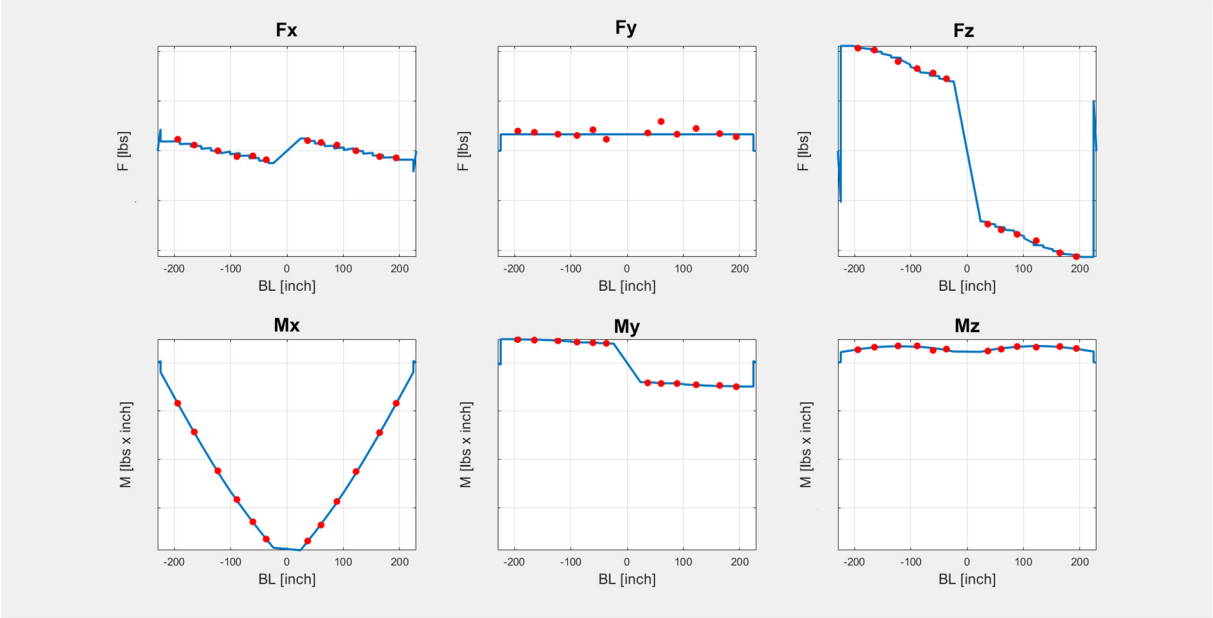

Figure 4. Low speed pull-up maneuver (airspeed = 0.11 V_D; helicopter mode): shear, bending and torsion diagrams (COLD conditions).

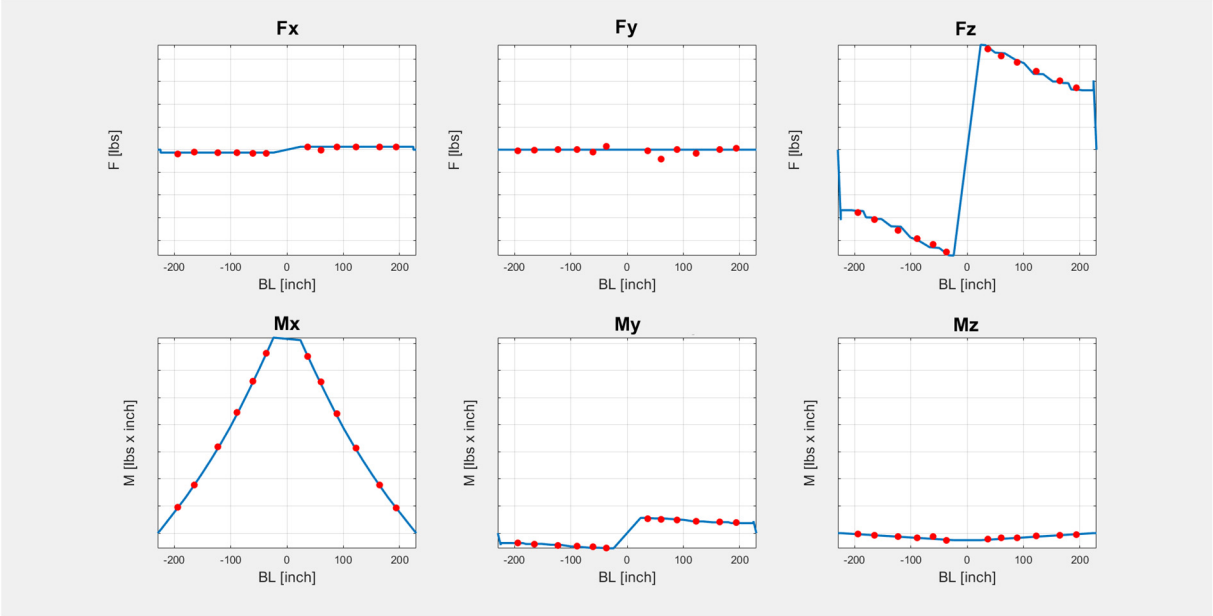

Figure 5. Taxi: shear, bending and torsion diagrams (COLD conditions).

For the first-phase optimization, all the 50 load conditions were used. For the second-phase optimization, a sub-set of the six most demanding loading conditions was used (Table 4).

Table 4. Most demanding loading conditions.

Load Case ID	Description	Wing Mass Condition	Nacelle Angle	Airspeed (V/V_D)
9	Symmetric Pull-up	Zero Fuel	90	0.42
12	Taxi	Full Fuel	95	0.00
13	Gust Condition	Full Fuel	0	0.43
15	Symmetric Pull-up	Full Fuel	95	0.41
17	Symmetric Pull-up	Zero Fuel	90	0.99
25	Rolling Pull-out	Full Fuel	30	1.06

3.1.3.4. Modifications to the Model Loading Strategy

The baseline Global FEM described in Section 3.1.3.1 was first converted into Altair Hypermesh compatible format, and subsequently it was necessary to avoid the use of INERTIA RELIEF, which resulted to be incompatible with buckling in Optistruct. Moreover, it was necessary to convert super-element matrices from op2 or output binary format to .pch format. The composite laminates PCOMP were converted into equivalent PSHELL. The equivalent PSHELL was chosen as the design variable, while the minimization of the mass is the design objective. The design constraints are set on buckling first eigenvalue, strains, wing tip displacements and rotations. A scheme of the process followed is shown in Figure 6.

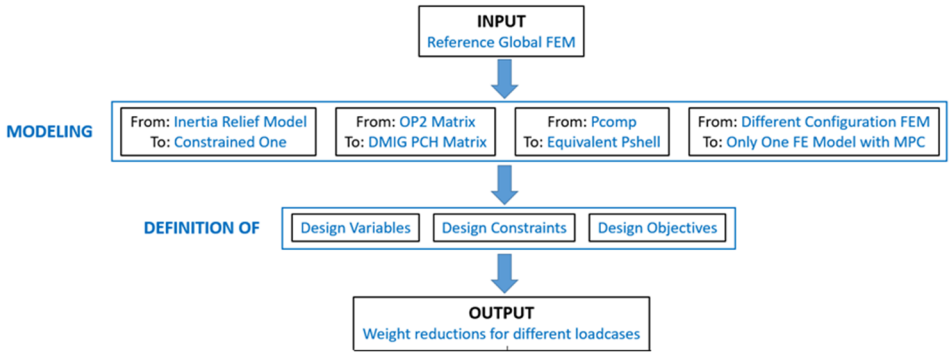

Figure 6. Optistruct optimization process.

As regards the modification needed to avoid the use of INERTIA RELIEF, the model was constrained at the SUPORT grid (CoG), and then linear and angular accelerations (previously calculated with the use of INERTIA RELIEF) were applied to the model to take into account inertial forces for the buckling runs.

Each of the loading conditions is characterized by a different position of the center of gravity, different fuel mass values, and different positions of the moveable surfaces and the tip masses. For this reason, to easily allow the program to select the appropriate mass conditions for each analyzed load case, it was necessary to define multipoint constraint equations for masses and CoG grids. Once the preparatory phase of the model is finished, the thicknesses associated with the equivalent PSHELL of the upper panel's skin, lower panel's skin and of the spar are selected as design variables, by imposing upper and lower limit values. Subsequently the response functions are defined: the first buckling eigenvalue, the torsional and flexural stiffness, and total structural mass. The final objective is the minimization of the mass (objective response). Different constrained optimization analyses were performed for the different design constraints.

3.1.4. Wing Stiffness Evaluation from FEM (Second Phase)

The wing Finite Element model resulting from the Optistrut optimization is then used to extract the wing stiffness properties of a beam-like model equivalent to the wing FEM in order to feed the aeroelastic stick-beam model. The evaluation of the wing stiffness

properties is based on static FE calculation with unitary loads (forces/moments) applied at the tip of the wing, having as output a set of nodal displacements at a certain number of wingspan stations. The calculation of equivalent beam properties is done by means of a 3D point cloud registration method [24]. The position and the displacements of the nodes corresponding to the selected wing stations were extracted from the BDF and PCH Nastran files for the un-deformed and deformed wing (for each one of the six load conditions: force and moment along each axis). Sections displacements and rotations were then calculated as the rigid motions (three translations and three rotations) of the un-deformed section that minimize the root mean square error between the FEM deformed and rigid displaced section points.

Relations between beam stiffness and section displacements can be obtained making use of the theory for Saint-Venant [24].

4. Preliminary Structural Design Results

4.1. Results of the Optimization Process and Flutter Analysis in the First Phase

The work already presented in [2] gives a number of solutions on the Pareto front, which can also be analyzed from a manufacturing point of view. In particular, the solution which guarantees the strength and buckling requirements at minimum mass and is feasible from a manufacturing point of view is selected for flutter analyses, and if cleared (flutter speed VF $\geq$ 1.15 times the Dive Speed, VD), it is further involved in the second-level optimization performed in this work, which is based on FE models.

4.2. Results of Finite Element Optimization (Second Phase) and Comparison with Respect to the Base Design

By performing dimensional optimizations in Optistruct, it is possible to obtain a wing-box with minimum weight, and optimal strength and flexural and torsional stiffness. The results obtained in terms of percentage of weight reduction with respect to the baseline model obtained in the first-level optimization for the main combinations of interest are reported in Table 5, where it is apparent that the more the objective functions considered, the less the weight reduction obtained.

Table 5. Results of Optistruct optimization in terms of percentage of delta weight with respect to the baseline obtained in the first-phase optimization.

Optimization	Delta-Weight (%)
Buckling	−26%
Buckling Stiffness (Out-of-plane flexural and Torsional)	−14%
Buckling Strength	−5%
Buckling Stiffness (In-plane and Out-of-plane flexural and Torsional) Strength	−3%

As an example, Figures 7 and 8 depict with different colors the thickness distribution of the upper and lower skin, for the buckling-optimized case, where the numbers represent the fraction with respect to the maximum thickness.

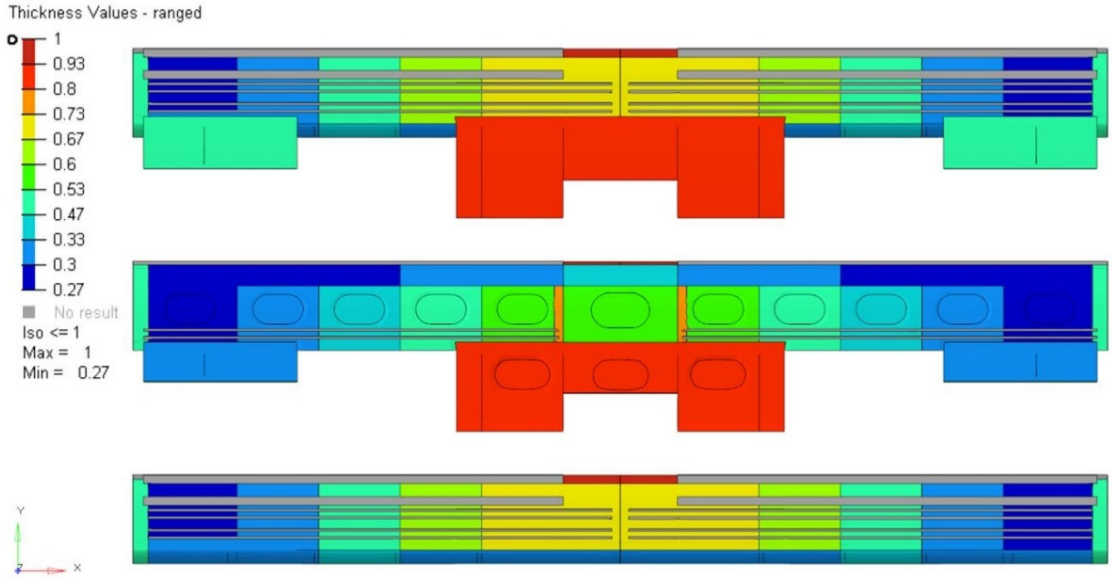

Figure 7. Upper and lower skin initial thickness distribution along wingspan.

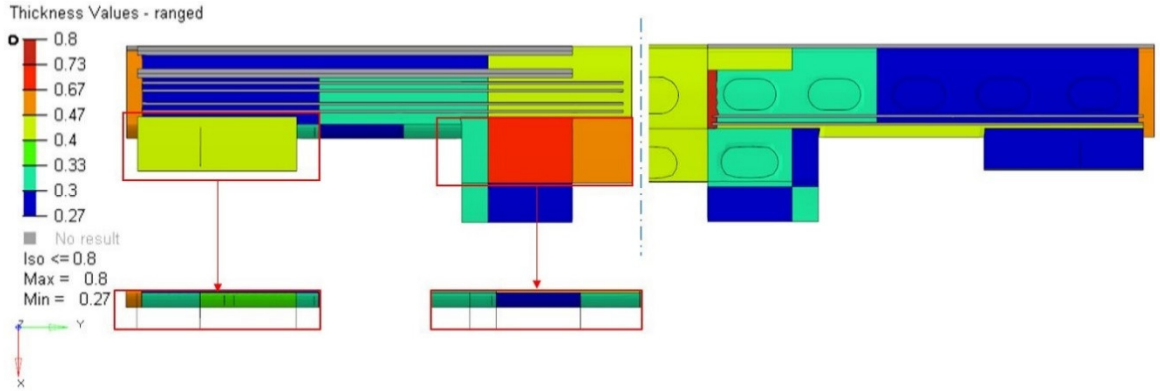

Figure 8. OptiStruct results: the different colors indicate different thickness of the wing zones.

Figures 9 and 10 depict the strains related to the same case (non-dimensional results).

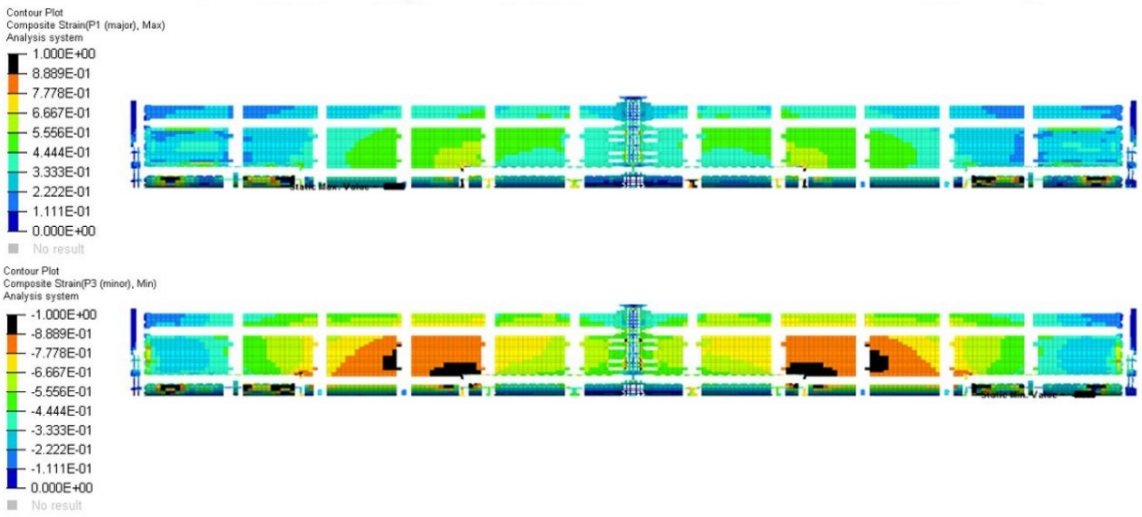

Figure 9. Contour plot of the upper skin strains (non-dimensional results).

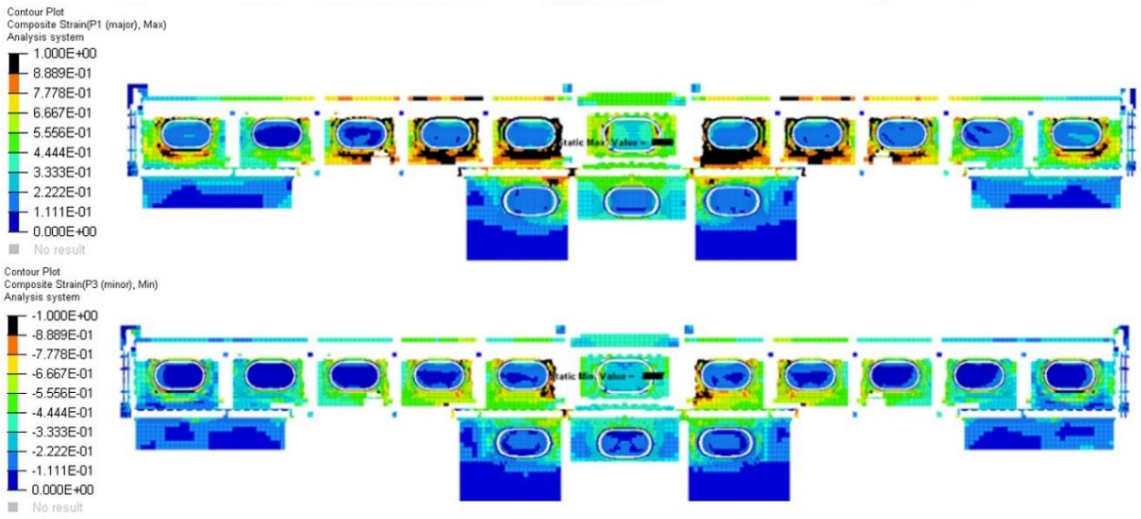

Figure 10. Contour plot of the lower skin strains (non-dimensional results).

4.3. Wing Stiffness Evaluation

Starting from the optimized configuration, the beam-like stiffness properties of the wing are evaluated (Section 3.1.4) and shown in Figure 11. The output of this calculation will be used for updating the aeroelastic model and then to perform the flutter calculation on the optimized configuration.

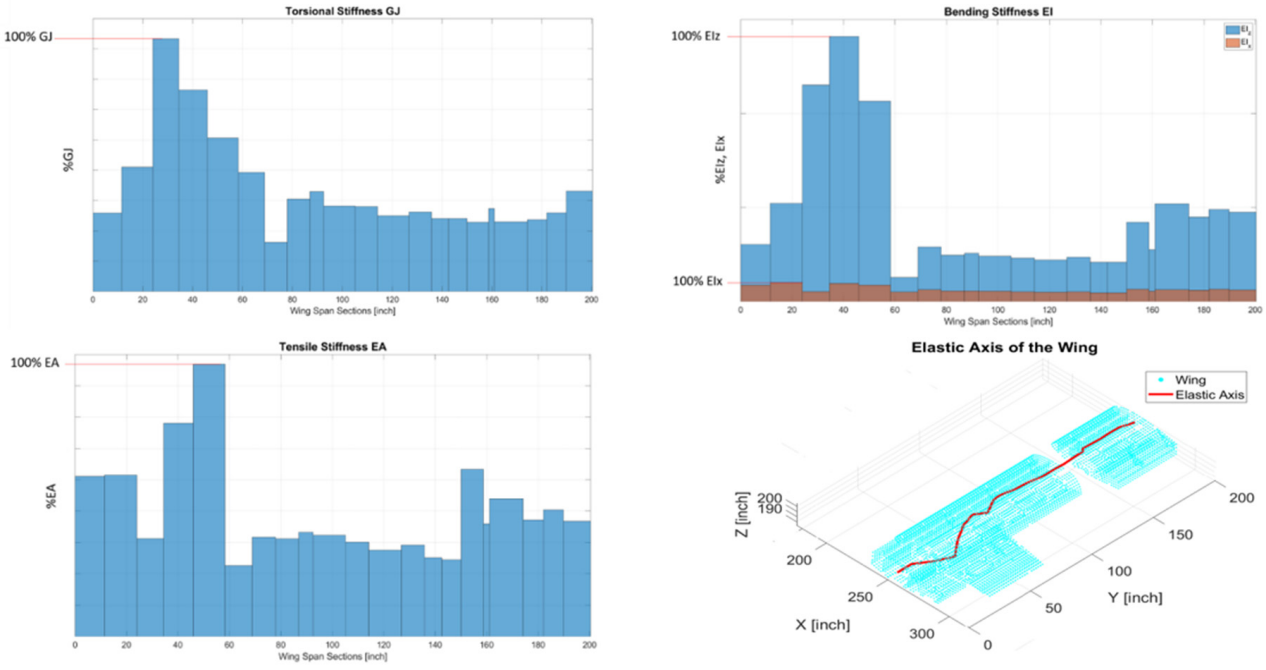

Figure 11. Wing stiffness properties and elastic axis position, to feed aeroelastic model.

4.4. Flutter Results Comparison

A schematic comparison between flutter results related to first-phase and second-phase optimizations is shown in Table 6.

Table 6. Comparison of flutter speed (ratio of flutter speed and dive speed) between first-phase and second-phase optimization.

Case Analyzed	First-Phase Optimized Wing	Second-Phase Optimized Wing
Full fuel case	1.52	1.67
Zero fuel case	1.48	1.63

With respect to the first-phase optimization, no changes in the flutter mechanisms have been detected. Due to the fact that the tail is the main driver of these flutter mechanisms, the only effect of the update of the wing structural properties, in line with the wing second-phase optimization, is a small increase of the flutter speed.

5. Higher Fidelity Models

The results of this two-level optimization, in terms of wing-box sizing, will be transferred into higher fidelity models (detailed FEM and digital mockup) to verify compliance with all the remaining requirements, such as stress and fatigue, crashworthiness, accessibility, assembly and integration, and manufacturability. After that, the final wing configuration will be launched for manufacturing. In Figure 12, an image of the digital mockup (DMU) is reported, which takes into account manufacturing, assembly, installation, accessibility to internal systems and maintenance constraints.

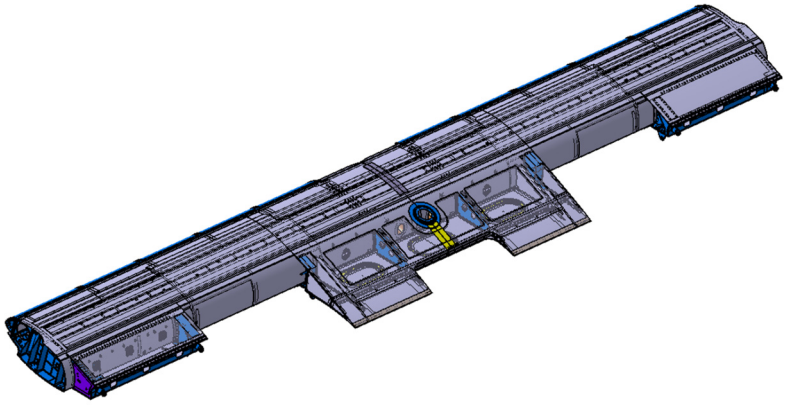

Figure 12. Wing Digital Mockup.

6. Conclusions

This work is a continuation of a former work by the authors [2]. The previous and the present works represent an overview of a two-level optimization of the composite wing of a tiltrotor. The main requirements underpinning the design of the wing have been presented, with a focus on the limitation on certain wing structural mode frequencies and aeroelastic clearance. The objective of the present paper is the description of the second part, i.e., second-level multi-objective optimization by using FE models (not engineering models as done in the former work). The problems (e.g., compatibility issues between Optistruct and Nastran INERTIA RELIEF) encountered in implementing such a process and the modification needed to the model have been described. The output of the process is the best solution—in terms of thickness—which minimizes the structural weight and is compliant with stiffness (flexural and torsional), strength and buckling requirements. The validation of the numerical methodology and tools could be delegated to other papers, using the preliminary results obtained in this work as a reference and the experimental results that will be achieved in the next project phases. The acquired experience with tiltrotor wing design allowed the authors to reduce the computational optimization effort by streamlining the set of sizing load conditions, which are quite different with respect to a fixed-wing aircraft. The optimal solution was then analyzed from a flutter point of view and results compared with previous outcomes, showing that the optimized wing structure

is flutter-free in the flight envelope. The results of this two-level optimization, in terms of wing-box sizing, will be transferred into higher fidelity models (detailed FEM and digital mockup) to verify compliance with all the remaining requirements, such as stress and fatigue, crashworthiness, accessibility, assembly and integration, and manufacturability. After that, the final wing configuration will be launched for manufacturing.

Author Contributions: All authors have equally contributed to this article. All authors have read and agreed to the published version of the manuscript.

Funding: This research was funded by the Clean Sky 2 Joint Undertaking under the European Union's Horizon 2020 research and innovation program under Grant Agreement number: 807090—FRC GAM 2018—H2020-IBA-CS2-GAMS-2017 Amendment Reference No. AMD-807090-23 [1].

Institutional Review Board Statement: Not Applicable.

Informed Consent Statement: Not Applicable.

Data Availability Statement: Not Applicable.

Conflicts of Interest: The authors declare no conflict of interest.

References

1. CLEAN SKY 2 Joint Undertaking Third Amended Bi-Annual Work Plan and Budget 2018–2019, Annex to decision CS-GB-2019-04-09 Decision Third Amended and Budget 2018–19. Available online: https://ec.europa.eu/research/participants/data/ref/h2020/other/wp/jtis/h2020-wp1819-cleansky_en.pdf (accessed on 1 April 2021).
2. Belardo, M.; Beretta, J.; Marano, A.D.; Diodati, G.; Paletta, N.; Di Palma, L. On the preliminary structural design strategy of the wing of the Next Generation Civil Tilt-Rotor Technology Demonstrator. *Int. J. Aeronaut. Space Sci.* **2020**. [CrossRef]
3. Park, J.-S.; Jung, S.N.; Lee, M.-K.; Kim, J.M. Design optimization framework for tiltrotor composite wings considering whirl flutter stability. *Compos. Part B Eng.* **2010**, *41*, 257–267. [CrossRef]
4. Kim, T.; Lim, J.; Shin, S.J.; Kim, D.-H. Structural Design Optimization of a Tiltrotor Aircraft Composite Wing to Enhance Whirl Flutter Stability. *Compos. Struct.* **2013**, *95*, 283–294. [CrossRef]
5. Belardo, M.; Paletta, N.; Di Palma, L.; Pecora, M. Structural and Aeroelastic Design of a Joined-Wing UAV. *J. Aerosp. Eng.* **2014**, *27*, 93–111. [CrossRef]
6. Paletta, N.; Belardo, M.; Di Palma, L. *Non-Linear Dynamic Loads Due to the Landing Impact of a Joined-Wing UAV*; SAE Technical Paper Series; SAE: Warrendale, PA, USA, 2011. [CrossRef]
7. Acree, C.W., Jr.; Johnson, W. Performance, Loads and Stability of Heavy Lift Tiltrotors. In Proceedings of the American Helicopter Society Vertical Lift Aircraft Design Conference, San Francisco, CA, USA, 18–20 January 2006.
8. Bielawa, R.L. *Rotary Wing Structural Dynamics and Aeroelasticity*, 2nd ed.; AIAA Publishing: Reston, VA, USA, 2006.
9. Johnson, W. *Dynamics of Tilting Proprotor Aircraft in Cruise Flight*; NASA Technical Note D-7677; NASA: Washington, DC, USA, 1974.
10. Moore, M.J.; Yablonski, M.J.; Mathew, B.; Liu, J. High Speed Tiltrotors: Dynamics Methodology. In Proceedings of the American Helicopter Society 49th International Annual Forum Proceedings, St. Louis, MO, USA, 19–21 May 1993.
11. Cecrdle, J. *Whirl Flutter of Turboprop Aircraft Structures*; Woodhead Publishing: Cambridge, UK, 2015.
12. Deb, K.; Pratap, A.; Agarwal, S.; Meyarivan, T. A fast and elitist multi-objective genetic algorithm: NSGA-II. *IEEE Trans. Evol. Comput.* **2002**, *6*, 182–197. [CrossRef]
13. Zhu, N.; O'Connor, I. iMASKO: A Genetic Algorithm Based Optimization Framework for Wireless Sensor Networks. *J. Sens. Actuator Netw.* **2013**, *2*, 675–699. [CrossRef]
14. Bruhn, E.F. *Analysis and Design of Flight Vehicle Structures*; Tri-State Offset Company: New York, NY, USA, 1973.
15. Albano, E.; Rodden, W.P. A Doublet-Lattice Method for Calculating Lift Distributions on Oscillating Surfaces in Subsonic Flows. *AIAA J.* **1969**, *7*, 279–285. [CrossRef]
16. Johnson, W. Calculation of Tiltrotor Aeroacoustic Model, Performance, Airloads, and Structural Loads. In Proceedings of the American Helicopter Society Aeromechanics Specialists's Meeting, Atlanta, GA, USA, 13–15 November 2000.
17. Harden, R.L.; Desmarais, R.N. Interpolation Using Surface Splines. *J. Aircr.* **1972**, *9*, 189–191. [CrossRef]
18. Loewer, S. Sensitivity of Tiltrotor High Speed Performance to Wing Structural Parameters. Diploma Thesis, Technische Universität Braunschweig, Braunschweig, Germany, 1992.

19. Altair Engineering. *Altair OptiStruct Verification Problems Manual—for NAFEMS, MacNeal-Harder, and Raasch Challenge Models*; Altair Engineering: Troy, MI, USA, 2017.
20. Lange, K. *Optimization*; Springer: New York, NY, USA, 2013.
21. Friedlander, M.P.; Macedo, I.; Pong, T.K. Gauge Optimization and Duality. *SIAM J. Optim.* **2014**, *24*, 1999–2022. [CrossRef]
22. Chiariello, A.; Orlando, S.; Vitale, P.; Linari, M.; Longobardi, R.; Di Palma, L. Development of smart morphing landing gear composite door for high speed compound rotorcraft. *Aerospace* **2020**, *7*, 88. [CrossRef]
23. Mora, H.; Mora-Pascual, J.M.; García-García, A.; Martínez-González, P. Computational Analysis of Distance Operators for the Iterative Closest Point Algorithm. *PLoS ONE* **2016**, *11*, e0164694. [CrossRef] [PubMed]
24. Drela, M. *ASWING 5.99 Technical Description—Steady Formulation*; 10 March 2015. Available online: https://web.mit.edu/drela/Public/web/aswing/asw_theory.pdf (accessed on 1 April 2021).